Molecular Cell, Volume *82*

Supplemental information

SETDB1/NSD-dependent H3K9me3/H3K36me3 dual heterochromatin maintains gene expression profiles by bookmarking poised enhancers

Amandine Barral, Gabrielle Pozo, Lucas Ducrot, Giorgio L. Papadopoulos, Sandrine Sauzet, Andrew J. Oldfield, Giacomo Cavalli, and Jérôme Déjardin

Figure S1: Co-occurrence of both H3K9me3 and H3K36me3 underlie a doubly modified chromatin, related to Figure 1

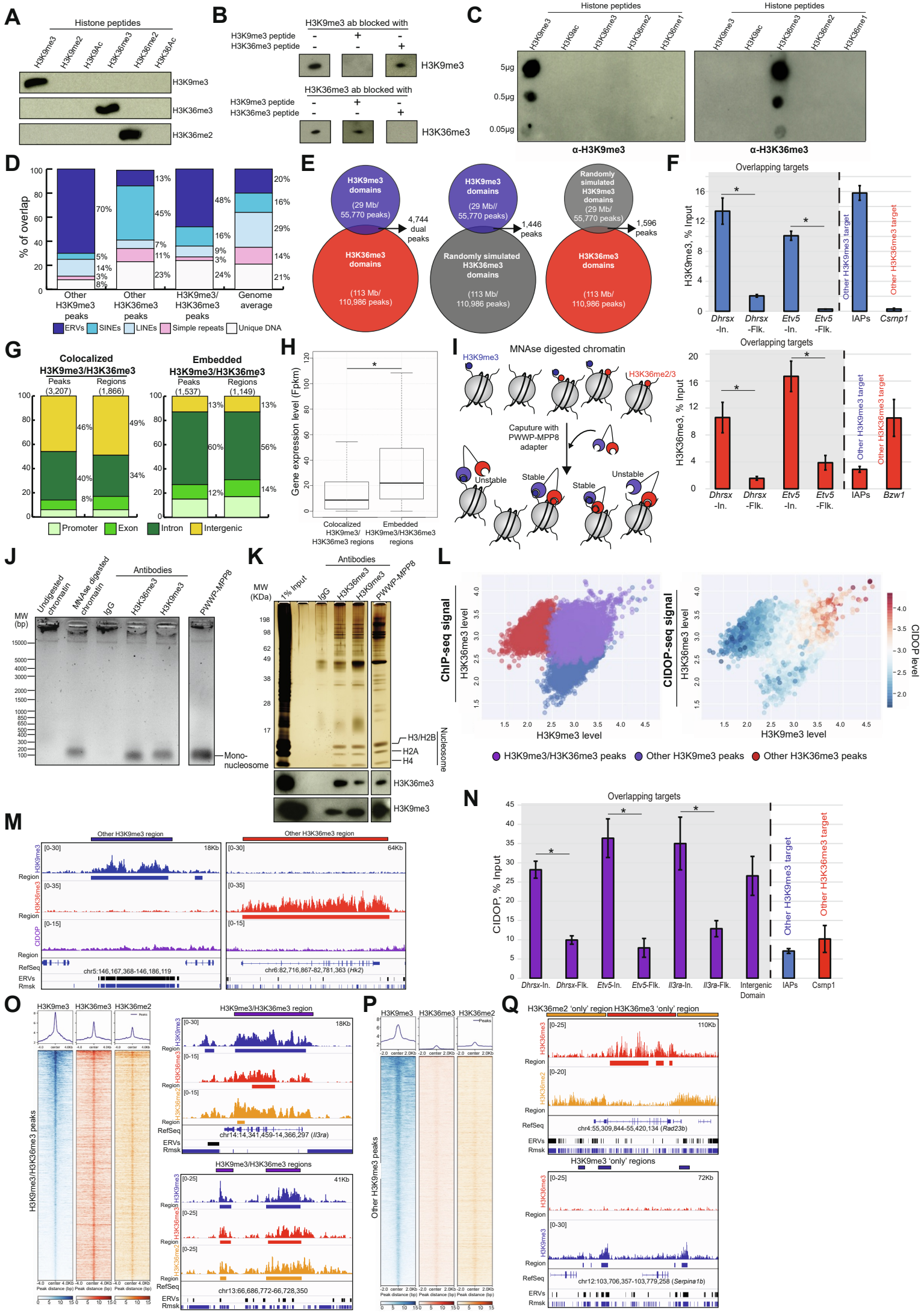

Figure S1: Co-occurrence of both H3K9me3 and H3K36me3 underlie a doubly modified chromatin, related to Figure 1. (A) Immunoblots performed on H3K9me3, H3K9me2, H3K9Ac, H3K36me3, H3K36me2 and H3K36Ac histone peptides and probed with the H3K9me3, H3K36me3 and H3K36me2 antibodies used in this study. **(B)** Immunoblots performed on nucleosomes extracted from ESCs. H3K9me3 and H3K36me3 antibodies were pre-incubated with H3K9me3 or H3K36me3 histone peptides to check for cross-reactivity. **(C)** Dot blots performed on H3K9me3, H3K9Ac, H3K36me3, H3K36me2, and H3K36me1 histone peptides probed with the H3K9me3 and H3K36me3 antibodies used in this study. **(D)** Histogram showing the contribution of distinct types of DNA repeats and unique sequences to regions enriched in H3K9me3 (other H3K9me3), H3K36me3 (other H3K36me3), both marks or their distribution in the genome (genome average). ERVs: LTR retrotransposons, SINEs: Short Interspersed Nuclear Elements, LINEs: Long Interspersed Nuclear Elements (LINEs), Simple repeats and Unique DNA. **(E)** Venn diagram showing the overlap between H3K9me3 peaks and H3K36me3 peaks (left), H3K9me3 peaks and randomly simulated H3K36me3 peaks (middle) or randomly simulated H3K9me3 peaks and H3K36me3 peaks (right). **(F)** ChIP-qPCR to measure the relative H3K9me3 fold-enrichment (blue, left) and H3K36me3 fold-enrichment (red, right) after input normalization inside positive H3K9me3/H3K36me3 regions (In.), or in Flanking regions (Flk), on Intracisternal A Particle (IAP, used as a H3K9me3 domain control) or on the *Csrnp1* transcribed gene body (used as a H3K36me3 domain control) (*: Student's T-test p-value < 0.05). **(G)** Histograms showing the genome-wide distribution of 'colocalized' H3K9me3/H3K36me3 domains (left) and 'embedded' H3K9me3/H3K36me3 domains (right). **(H)** Box-plot showing the expression level (Fpkm) of genes containing 'colocalized' H3K9me3/H3K36me3 domains or 'embedded' H3K9me3/H3K36me3 domains. (Wilcoxson signed rank test: * p-value = $2.2*10^{-16}$). **(I)** Model detailing the Chromatin Interacting DOmain Precipitation approach (CIDOP). After MNAse digestion, mononucleosomes were captured with the PWWP-MPP8 adapter protein. The PWWP-MPP8 adapter captures H3K9me3/H3K36me3 doubly modified nucleosomes and associated DNA. The PWWP-MPP8 adaptor does not stably bind to

nucleosomes only bearing H3K9me3 or H3K36me3. **(J)** Ethidium Bromide staining of agarose gel tracking mononucleosome immunoprecipitation with IgG, H3K9me3, H3K36me3 antibodies or the PWWP-MPP8 adapter. PWWP-MPP8 adapter captures DNA fragments of ~150bp in size. **(K)** Silver staining (top) and H3K9me3 or H3K36me3 immunoblots (bottom) on immunoprecipitated mononucleosomes using IgG, H3K9me3, H3K36me3 antibodies or the PWWP-MPP8 adapter. **(L)** Left: scatter-plot showing the distribution of H3K9me3/H3K36me3 regions, other H3K9me3 regions and other H3K36me3 regions according to their enrichment levels obtained by ChIP-seq. Right: scatter-plot showing the enrichment of CIDOP-seq signal, overlaid on the above ChIP-seq scatter-plot. **(M)** Genome browser tracks of H3K9me3 (blue), H3K36me3 (red) and CIDOP (purple) on another H3K9me3 region (left) and another H3K36me3 region (right). **(N)** CIDOP qPCR to measure the relative CIDOP fold-enrichment after input normalization inside positive H3K9me3/H3K36me3 regions (In.), or in Flanking regions (Flk), on Intracisternal A Particle (IAP, used as a H3K9me3 domain control) or on the *Csrnp1* transcribed gene body (used as a H3K36me3 domain control) (*: Student's T-test p-value < 0.05). **(O)** Heatmap showing the distributions of H3K9me3 (blue), H3K36me3 (red) and of H3K36me2 (orange) on H3K9me3/H3K36me3 regions (left). Genome browser tracks of H3K9me3 (blue), H3K36me3 (red) and H3K36me2 (orange) on H3K9me3/H3K36me3 regions (right). **(P)** Heatmap showing H3K9me3 (blue), H3K36me3 (red) and H3K36me2 (orange) distributions on other H3K9me3 regions. **(Q)** Genome browser tracks of H3K36me3 (red) and H3K36me2 (orange) on H3K36me3 'only' region and H3K36me2 'only' regions.

Figure S2: H3K9me3/H3K36me3 domains are not bivalent, related to Figure 2

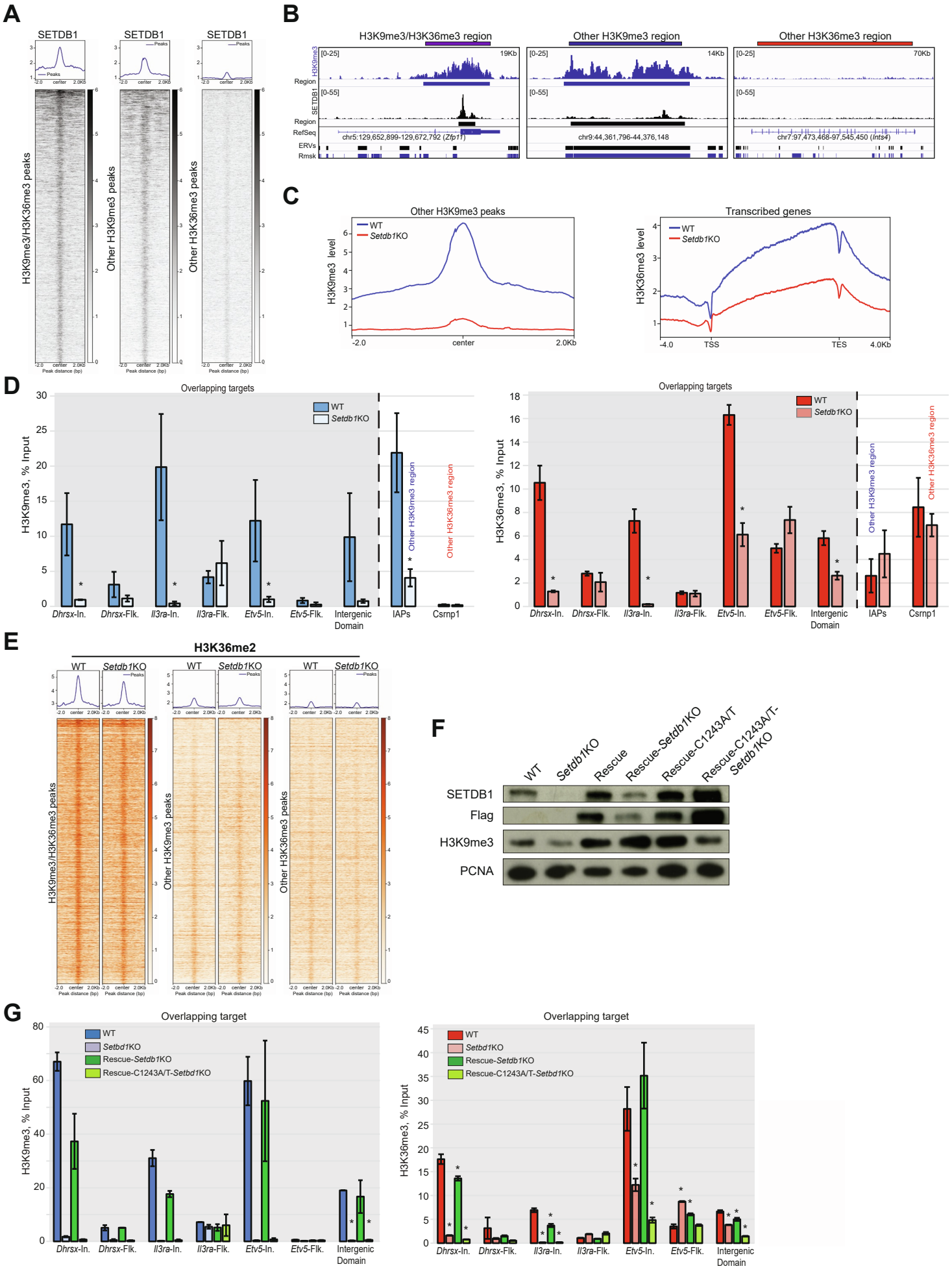

Figure S2: H3K9me3/H3K36me3domains are not bivalent, related to Figure 2.

(A) Heatmaps showing the distribution of SETDB1 on H3K9me3/H3K36me3 regions as compared to other H3K9me3 regions or other H3K36me3 regions. **(B)** Genome browser tracks of H3K9me3 (blue) and SETDB1 (black) on H3K9me3/H3K36me3 regions and on other H3K9me3 regions or other H3K36me3 regions. **(C)** Metaplots showing H3K9me3 levels on H3K9me3 regions (left) and H3K36me3 levels on transcribed gene (right) in WT and in *Setdb1* KO cells. **(D)** ChIP-qPCR to measure the relative H3K9me3 fold-enrichment (blue, left) and H3K36me3 fold-enrichment (red, right) after input normalization inside positive H3K9me3/H3K36me3 regions (In.), or in Flanking regions (Flk), on Intracisternal A Particle (IAP, used as a H3K9me3 domain control) or on the *Csrnp1* transcribed gene body (used as a H3K36me3 domain control) in WT, *Setdb1* KO cells (*: Student's T-test p-value < 0.05). **(E)** Heatmaps showing H3K36me2 enrichment on dual domains, on other H3K9me3 regions or other H3K36me3 regions in WT and *Setdb1* KO cells. (Wilcoxson signed rank test: *: p-value = $6.83*10^{-3}$; $4.95*10^{-3}$; $2.78*10^{-4}$ on dual domains, other H3K9me3 regions and other H3K36me3 regions, respectively). **(F)** SETDB1, Flag, H3K9me3 and PCNA immunoblots performed on nuclear extracts from WT, *Setdb1* KO, Rescue-*Setdb1*KO and Rescue-C1243A/T-*Setdb1*KO cells. **(G)** ChIP-qPCR to measure the relative H3K9me3 fold-enrichment (blue, left) and H3K36me3 fold-enrichment (red, right) after input normalization inside positive H3K9me3/H3K36me3 regions (In.), or in Flanking regions (Flk) in WT, *Setdb1* KO cells, Rescue-*Setdb1*KO and Rescue-C1243A/T-*Setdb1*KO cells. (*: Student's T-test p-value < 0.05).

Figure S3: SETD2 is not critically involved in H3K36me3 on dual domains in mESCs and in MSCs, related to Figure 3

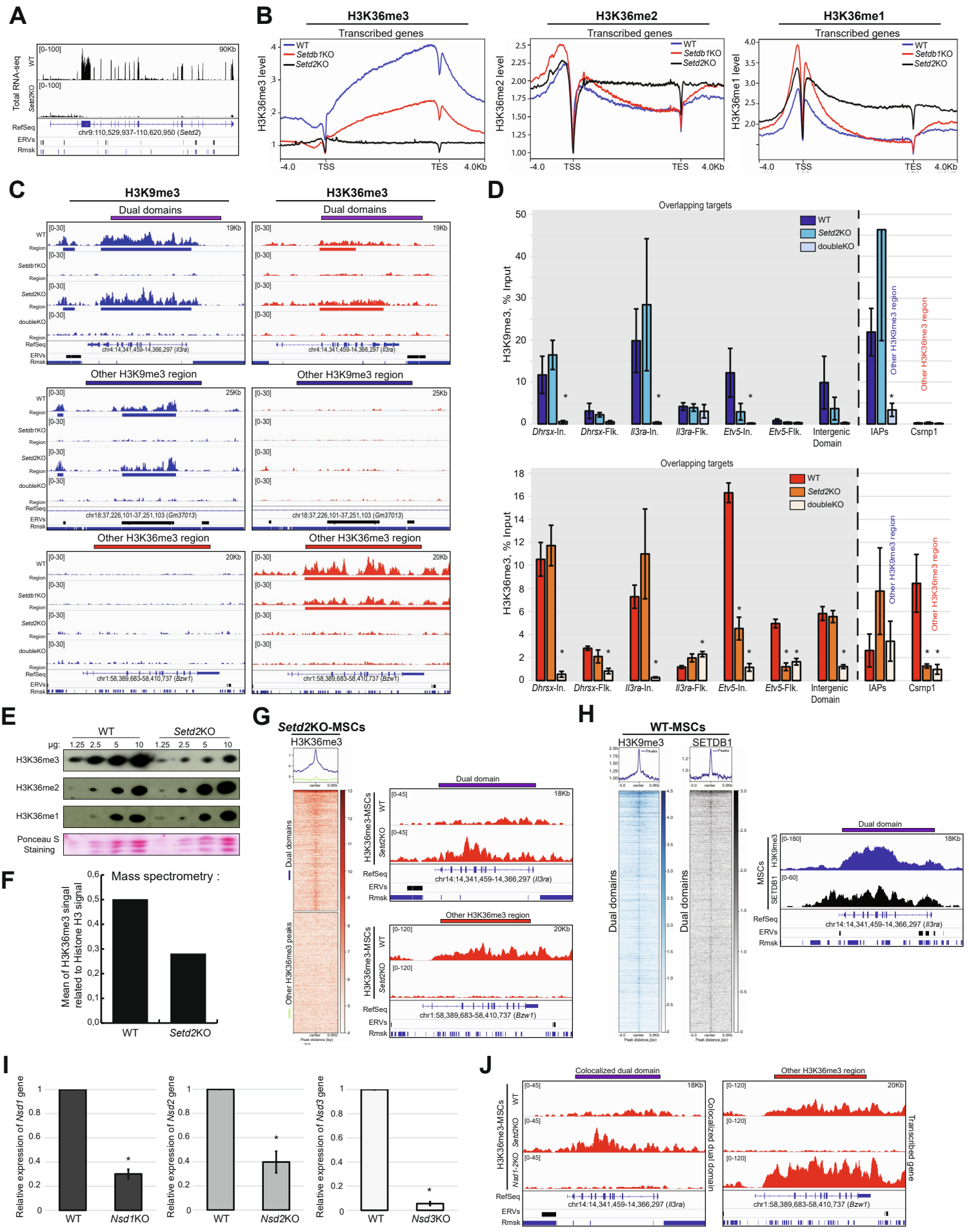

Figure S3: SETD2 is not critically involved in H3K36me3 on dual domains in mESCs and in MSCs related to Figure 3.

(A) Genome browser tracks of total RNA-seq in WT and *Setd2* KO cells. **(B)** Metaplots showing H3K36me3, H3K36me2 and H3K36me1 levels on transcribed genes in WT, *Setdb1* KO and *Setd2* KO cells. **(C)** Genome browser tracks of H3K9me3 (blue) and H3K36me3 (red) on H3K9me3/H3K36me3 regions compared with other H3K9me3 or H3K36me3 regions in WT, *Setdb1* KO, *Setd2* KO and double KO cells. **(D)** ChIP-qPCR to measure the relative H3K9me3 fold-enrichment (top) and H3K36me3 fold-enrichment (bottom) after input normalization inside positive H3K9me3/H3K36me3 regions (In.), or in Flanking regions (Flk), on Intracisternal A Particle (IAP, used as a H3K9me3 domain control) or on the *Csrnp1* transcribed gene body (used as a H3K36me3 domain control) in WT, *Setdb2* and double KO cells (*: Student's T-test p-value < 0.05). **(F)** Histogram showing the percentage of H3K36me3 related to histone H3 in WT and *Setd2* KO cells. **(G)** Left: heatmap showing H3K36me3 enrichment on dual domains and on other H3K36me3 regions (i.e. transcribed gene bodies) in *Setd2* KO mesenchymal stem cells (MSCs) Right: genome browser tracks of H3K36me3 on a dual domain and on another H3K36me3 region in WT and *Setd2* KO MSCs. **(E)** Top: H3K36me3, H3K36me2, H3K36me1 immunoblots from WT and *Setd2*KO cells. Bottom: Ponceau S staining from WT and *Setd2*KO cells. **(H)** Heatmaps showing H3K9me3 (blue) and SETDB1 (black) enrichments on dual domains in MSCs. Right: Genome browser tracks of H3K9me3 (blue) and SETDB1 (black) on a dual domain in MSCs (Matsumura et al., 2015). **(I)** qRT-PCR to measure the relative expression level of *Nsd1* (left), *Nsd2* (middle), *Nsd3* (right) genes after *Actin* normalization in Nsd1KO, Nsd2KO, Nsd3KO cells, respectively. (Student's T-test p-value < 0.05) **(J)** Genome browser track of H3K36me3 on an 'embedded' dual domain, on a 'colocalized' dual domain on another H3K36me3 region, in WT, *Setd2* KO and *Nsd1; Nsd2 double* KO MSCs.

Figure S4: Dual domain destabilization does not reactivate alternative promoters, related to Figure 4

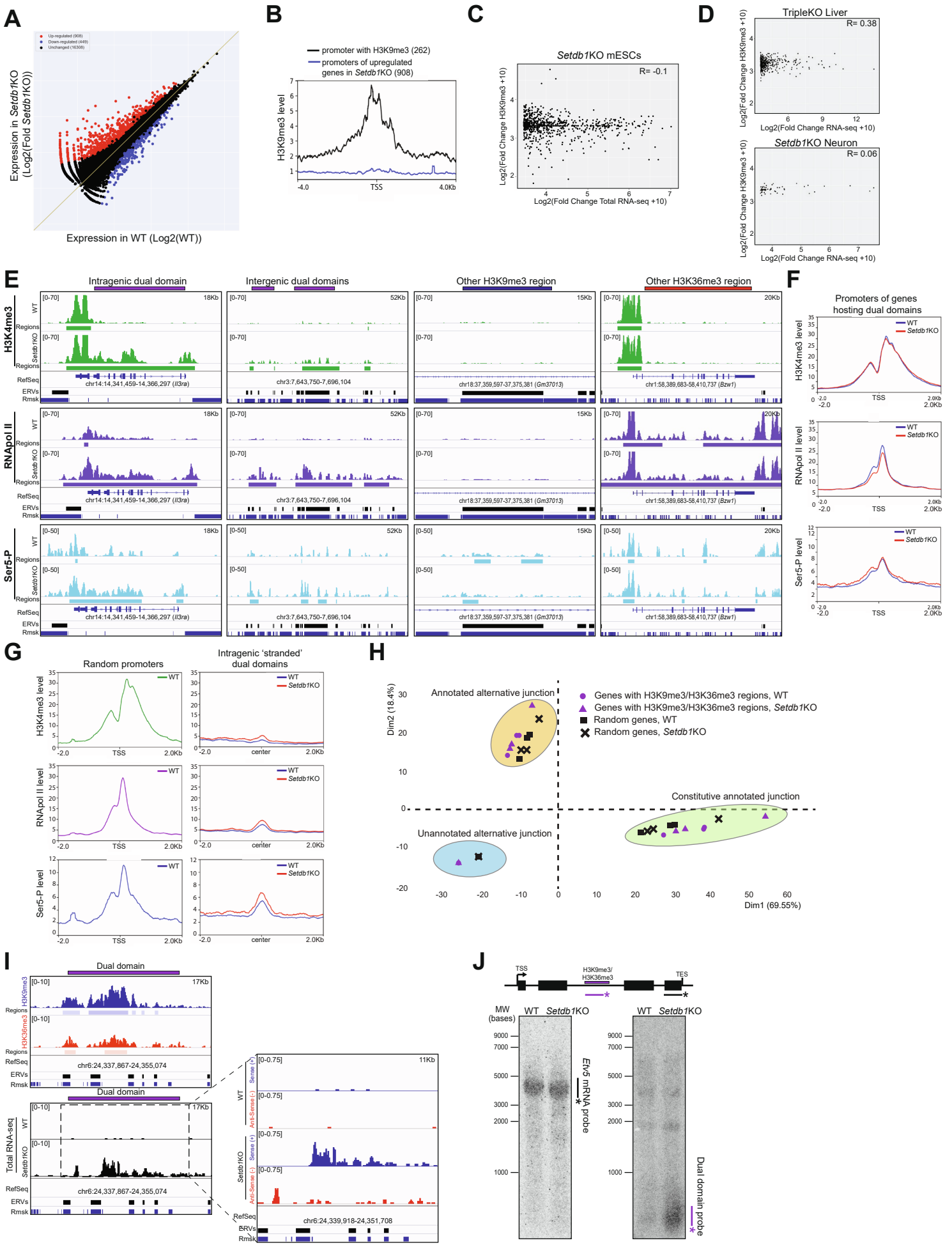

Figure S4: Dual domain destabilization does not reactivate alternative promoters, related to Figure 4.

(A) Scatter-plot showing the expression levels log2 Fold change of all Ref Seq genes in WT or *Setdb1* KO cells. In absence of SETDB1, 908 genes are upregulated (red), 16308 genes are unchanged (black) and 449 genes are downregulated (blue). **(B)** Metaplot showing the level of H3K9me3 on promoters containing H3K9me3 mark and on promoters of upregulated genes in *Setdb1* KO cell. **(C)** Scatter plot showing the correlation between H3K9me3 level on promoters of upregulated genes in *Setdb1* KO cells and their expression level. The spearman correlation is shown. **(D)** Scatter plot showing the correlation between H3K9me3 level on promoters and expression level of upregulated genes in TripleKO liver cells (top) and in *Setdb1* KO neuronal cells. The spearman correlation is shown. **(E)** Genome browser tracks showing H3K4me3, RNApol II and Serine 5 (Ser5-P) on an intragenic and intergenic dual domain and on another H3K9me3 region or another H3K36me3 regionin WT and *Setdb1* KO cels. **(F)** Metaplots of H3K4me3, RNApol II and Serine-5 (Ser5-P) levels on promoters of genes hosting dual domains in WT and *Setdb1* KO cells. **(G)** Metaplots of H3K4me3, RNApol or Serine 5 (Ser5-P) levels on promoters (random promoters were selected according to ± 2Kb regions from transcription start site of Refseq genes) in WT (left) and on intragenic dual domains in WT and *Setdb1* KO cells (right) Promoters and intragenic dual domains are stranded according to strand of their hosting RefSeq genes. **(H)** Principal component analysis (PCA) of constitutive annotated junction (green circle), annotated alternative junction (yellow circle) and unannotated alternative junction (blue circle) on genes containing dual domains (purple) and random genes (black) in WT and *Setdb1* KO cell lines. **(I)** Top: genome browser tracks of H3K9me3 and H3K36me3 on a dual domain. Bottom: genome browser tracks of total RNA-seq (black) of a dual domain in WT and *Setdb1* KO cell lines (left). Genome browser tracks of sense strand (blue) and anti-sense strand (red) of a dual domain in WT and *Setdb1* KO cell lines. **(J)** Top: scheme showing the design of Northern-blot probes. Bottom: northern-blot using mRNA probe (left) or dual domain probe (right) in WT or *Setdb1* KO cells.

Figure S5: Destabilized dual domains gain enhancer hallmarks, related to Figure 5

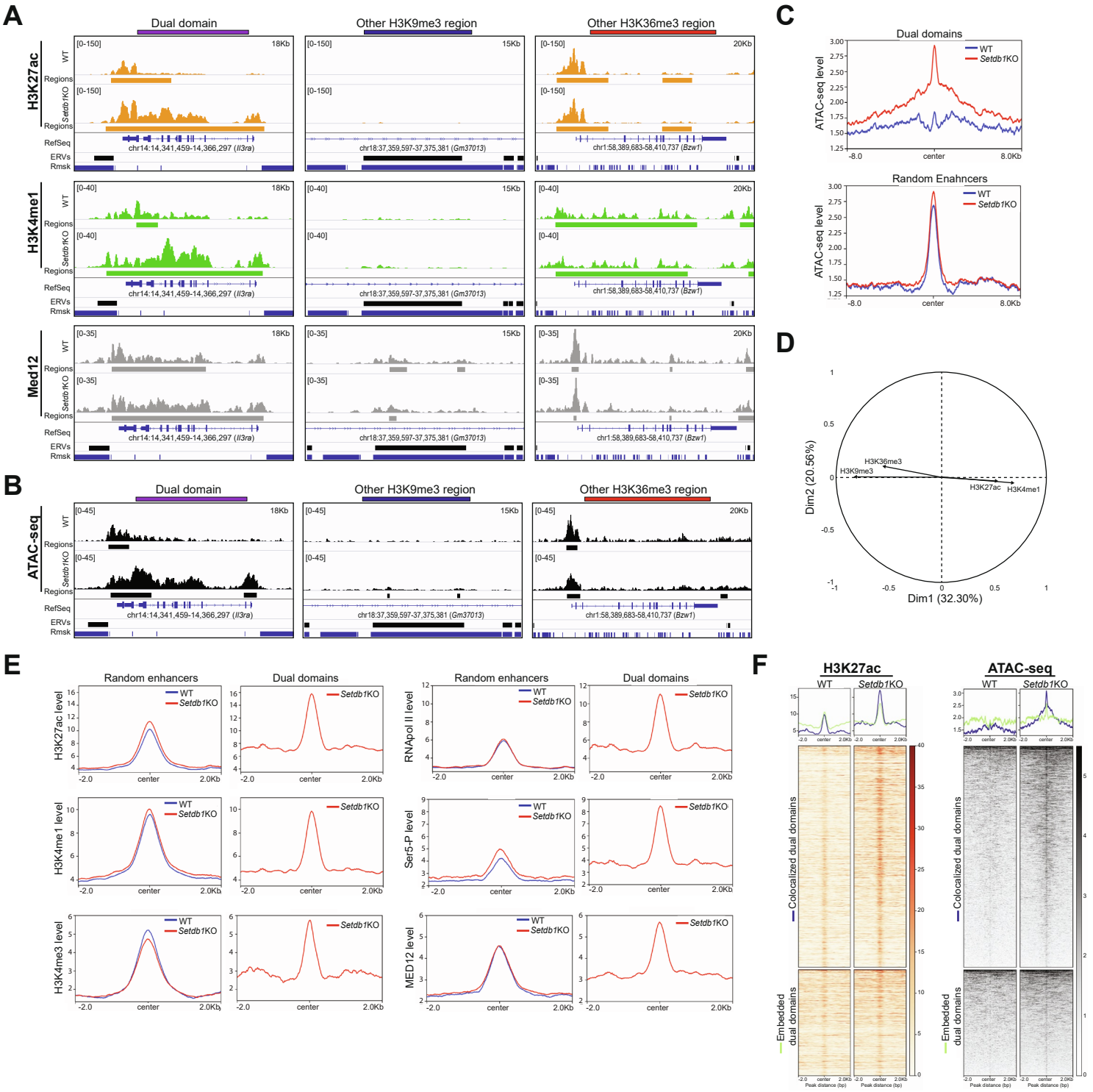

Figure S5: Destabilized dual domains gain enhancer hallmarks, related to Figure 5.

(A) Genome browser tracks showing H3K27ac, H3K4me1 and MED12 on a dual domain, on another H3K9me3 region or another H3K36me3 region in WT and *Setdb1* KO cells. **(B)** Genome browser tracks of ATAC-seq on dual regions, on other H3K9me3 regions and on other H3K36me3 regions in WT and *Setdb1* KO cells. **(C)** Metaplots of ATAC-seq signal levels on dual domains and on other enhancers (random enhancers were selected according to H3K27Ac peaks which did not map to known promoter regions) in WT and *Setdb1* KO cells. (Wilcoxson signed rank test: *: p-value < $2.2*10^{-16}$ on dual domains. p-value = 3.08*10-5 on random enhancers) **(D)** Principal component analysis (PCA) performed using H3K9me3, H3K36me3, H3K27ac, H3K4me1 levels on dual domains in WT vs *Setdb1* KO cells. **(E)** Metaplot showing H3K27ac, H3K4me1, H3K4me3, RNApol II, Serine 5 (Ser5-P) and MED12 levels on random enhancers in WT and *Setdb1* KO cells (left) and on dual regions in *Setdb1* KO cell line (right). **(F)** Heatmaps showing H3K27ac and ATAC-seq distributions on colocalized and embedded dual domains in WT and *Setdb1*KO cells.

Figure S6: Loss of SETDB1 does not alter overall TAD structure, related to Figure 6

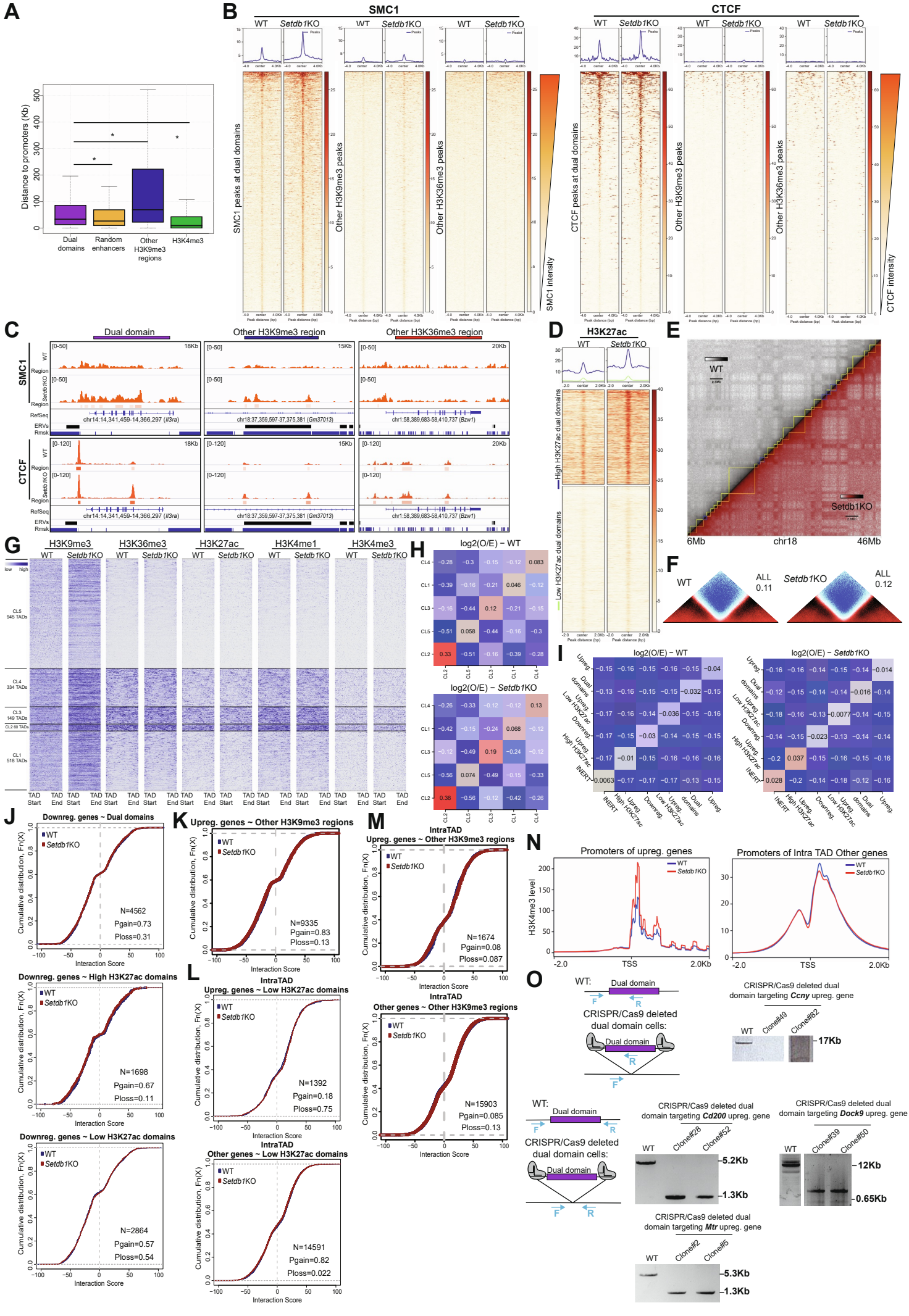

Figure S6: Loss of SETDB1 does not alter overall TAD structures, related to Figure 6.

(A) Box-plot showing the distance to promoters of dual domains, random enhancers, other H3K9me3 regions and of H3K4me3 regions. (Wilcoxson signed rank test: *: p-value < $2.2*10^{-16}$) **(B)** Heatmaps showing SMC1 (left) and CTCF (right) enrichment on dual domains and on other H3K9me3 regions or other H3K36me3 regions in WT and *Setdb1* KO cells. Heatmaps ranked according to the SMC1 and CTCF signal intensity in *Setdb1* KO cells, respectively. (Wilcoxson signed rank test: *: p-value = $3.75*10^{-3}$ and p-value < $2.2*10^{-16}$ on dual domains for CTCF and SMC1, respectively. n.s on other H3K9me3 and H3K36me3 regions for CTCF and SMC1) **(C)** Genome browser tracks showing CTCF and SMC1 on a dual domain, on another H3K9me3 region or another H3K36me3 region in WT and *Setdb1* KO cells. **(D)** Heatmap showing H3K27ac enrichment on high H3K27ac and low H3K27ac dual domains in WT and *Setdb1* KO cells. **(E)** Hi-C matrices representing non-normalized observed interaction counts (log2) for the WT (upper left triangle, greyscale) and Setdb1 KO (lower right triangle, grey/red/black scale) for a large genomic *locus* of chromosome 18. TAD calls in WT cells are highlighted in yellow whereas TAD calls in Setdb1 KO are highlighted in orange. WT TADs harbouring upregulated genes and dual domains are highlighted in blue. **(F)** Average boundary profiles for WT (top) and *Setdb1* KO (bottom) cells representing log2(Observed/Expected) ratios for each bin across all regions. The average window size spans 250kb upstream and downstream of each called boundary at a resolution of 500bp. **(G)** Genome wide WT TAD segmentation based on average enrichment of epigenetic marks in WT and *Setdb1* KO cells across the full TAD length (kmeans). For representation, each TAD was split into 300 bins of equal size (depending on the TAD size) and the average enrichment of each mark across each bin is used for plotting. **(H)** Quantification of interaction enrichment between all pairs of epigenetically segmented TADs calculated as the ratio of Observed/Expected interactions across all pairs (log2). Interactions occurring at more than 50Mb genomic distance and intraTAD self-interactions are excluded from the analyses. **(I)** Quantification of interaction enrichment between all pairs of TADs classified based on the overlaps with mis-regulated

genes and dual domains. TADs that do not overlap with any of these features are characterized as INERT. **(J)** Empirical distribution functions illustrating the interaction strength dynamics upon SETDB1 depletion between downregulated genes and dual domains (top), high H3K27ac domains (middle) and low H3K27ac domains (bottom). (KS one-sided test: p= n.s. for all dual domains, high and low H3K27ac domains, respectively). **(K)** Empirical distribution functions illustrating the interaction strength dynamics upon SETDB1 depletion between upregulated genes and other H3K9me3 regions. (KS one-sided test: p= n.s.). **(L)** Estimation of intra-TAD target gene specificity of dual domains with low levels of H3K27Ac by comparing interaction dynamics between upregulated genes (top) and all the other genes in the same TAD (bottom). (KS one-sided test: p= n.s. for upregulated genes and others genes, respectively) **(M)** Estimation of intraTAD target gene specificity of dual domains with other H3K9me3 regions by comparing interaction dynamics between upregulated genes (top) and all the other genes in the same TAD (bottom). (KS one-sided test: p= n.s. for upregulated genes and others genes, respectively). **(N)** Metaplot showing H3K4me3 levels on the promoters of upregulated genes (left) and of all the other genes within the same TAD (IntraTAD other genes, right) in WT and *Setdb1*KO cells. **(N)** Left: Scheme detailing PCR primers used to screen CRISPR/Cas9 deleted dual domains. Right: Ethidium Bromide staining of agarose gels tracking PCR product sizes after CRISPR/Cas9 dual domain deletion.

Figure S7: Dual domains do not randomly overlap with enhancers in embryonic and adult tissues, related to Figure 7

A

Transcription factors	Motif	Number of dual domains	p-values
RXR (Retinoid X receptor)		174	1.5*10^-1206
FOSL (AP1)		239	1.5*10^-1206
TBX (T-box factor)		106	3.3*10^-381
ELF (Ets-related factor)		96	1.2*10^-119
ETV (Ets-related factor)		17	2.4*10^-88
Myc		134	2.6*10^-93
SMAD (TGF-pathway)		228	2.2*10^-235
NeuroG2		97	4.4*10^-63
EGR (Ets-related factor)		344	1.7*10^-51
SOX/SRY (Sry-box gene)		513	2.6*10^-93
FOX (Forkhead-box factors)		168	2.6*10^-93
NFY (Nuclear factor Y)		39	4.7*10^-15
KLF/SP (Krüpple-like factor)		490	5.7*10^-314
TFAP2 (AP2)		834	1.3*10^-231
Hox (Hox-related factors)		62	1.4*10^-28
Nkx (Homebox factor)	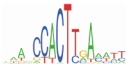	176	4.7*10^-176

B

Tissues	Enhancers	Overlaps of simulated: Dual domains	Overlaps of simulated: All other H3K9me3 regions	Z-score: Dual domains	Z-score: All other H3K9me3 regions	Tissue-specifc Enhancers	Overlaps of simulated: Dual domains	Overlaps of simulated: All other H3K9me3 regions	Z-score: Dual domains	Z-score: All other H3K9me3 regions	
Cortex	53,964	87	1098	6.1	21.6	20,485	29	371	1.6	12.5	Adult tissues (8 weeks)
Olfact bulb	60,891	104	1297	5.9	22.4	26,641	39	496	0.2	4.4	
Thymus	22,095	40	502	13.6	1.1	5,722	8	108	5.4	0.6	
Bone marrow	38,807	62	786	20.0	34.8	11,468	15	194	10.8	12.7	
Spleen	45,358	78	973	16.4	5.9	24,793	13	163	8.1	2.2	
Small Intestine	66,693	120	1494	18.9	9.9	9,747	39	494	3.6	12.2	
Brown adipose	79,154	138	1724	14.7	17.9	33,296	48	612	5.1	65.9	
Placenta	70,423	119	1492	23.8	10.4	33,531	50	635	17.5	1.9	
Testis	24,242	37	467	10.3	2.7	9,613	14	178	6.9	11.9	
Forebrain	30,385	86	1021	3.0	21.3	9,571	20	246	0.6	11.3	Embryonic tissues (15.5 days)
Hindbrain	26,873	52	638	2.8	17.9	7,102	9	118	0.2	7.6	
Midbrain	24,572	65	772	0.7	18.3	4,622	8	98	1.5	5.5	
Neural tube	24,248	45	553	3.0	15.8	4,359	5	69	0.7	5.1	
Heart	43,348	94	1143	5.3	19.6	17,747	31	385	2.2	11.7	
Lung	35,828	70	869	6.7	16.0	10,408	15	194	3.3	6.9	
Liver	20,931	45	545	8.8	11.0	14,547	21	260	4.2	7.6	
Kidney	41,763	80	982	7.3	16.9	11,198	21	269	7.7	7.8	
Intestine	18,880	32	400	8.1	10.6	2,656	3	44	0.8	3.0	
Stomach	23,981	42	522	5.0	13.3	2,882	3	46	4.4	4.8	
Limb	22,200	40	493	4.3	11.8	5,464	7	94	0.4	4.6	

C

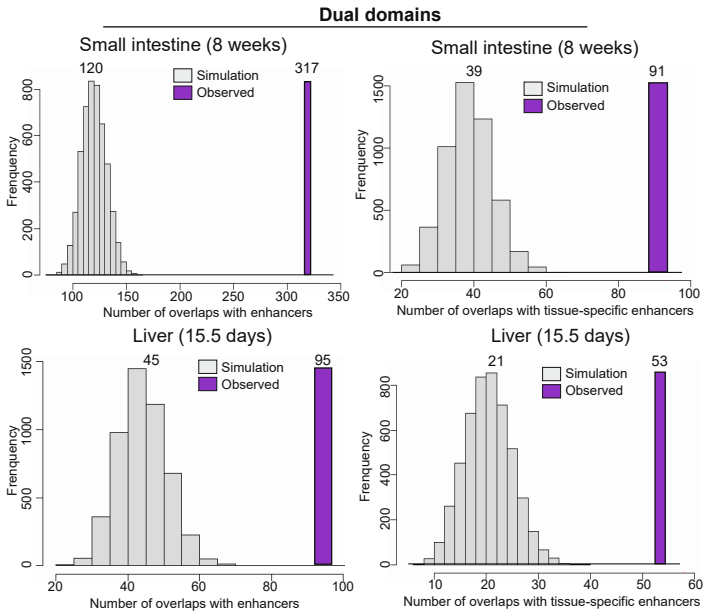

D

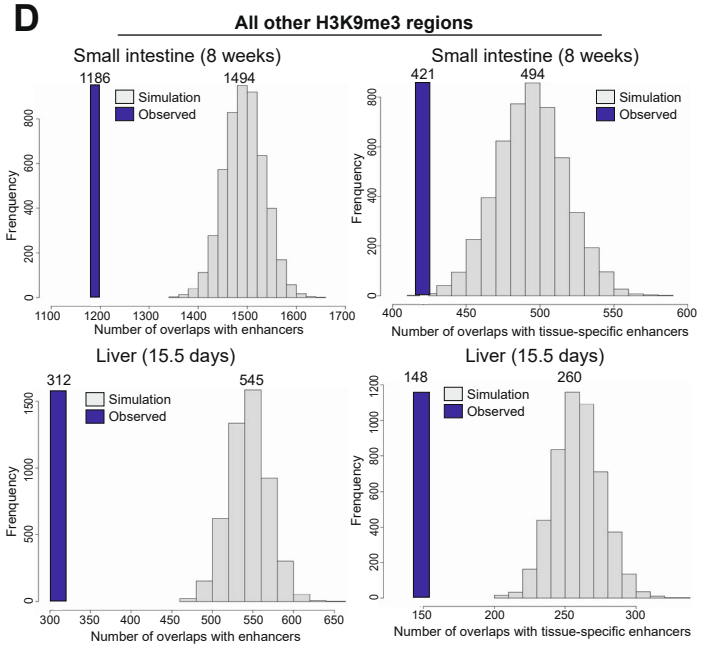

Figure S7: Dual domains do not randomly overlap with enhancers in embryonic and adult tissues, related to Figure 7.

(A) Transcription factor motifs enriched within dual domains. (**B**) Tables showing the simulation of overlaps between enhancers (left) or tissue-specific enhancers (right) with randomly selected dual domains or all other H3K9me3 regions in adult tissues (top) and embryonic tissues (bottom) Z-score is the number of standard deviations from the mean of simulated overlap. Z-scores in green shown a correlation and an anti-correlation in red **(C)** Histograms showing average overlap of enhancer with dual domains (observed, purple) and randomly selected regions (simulation, grey) in adult tissues (small intestine) and in embryonic tissues (liver). **(D)** Histograms showing average overlap of enhancer with all other H3K9me3 region (observed, blue) and randomly selected regions (simulation, grey) in adult tissues (small intestine) and in embryonic tissues (liver).

Table S1. List of oligonucleotides used in this study, related to Figures 1, 2, 3, 4, 5 and 6.

Sequence (5' to 3')	Primer name	Used for
CCTGTGCCTTCCAGGTCAAT	Dhrsx-In-FOR	ChIP and CIDOP-qPCR
GGAACGTTTTTCCCACTGCG	Dhrsx-In-REV	ChIP and CIDOP-qPCR
GCTTTGCCAATTCGGACCTC	Dhrsx-Flk-FOR	ChIP and CIDOP-qPCR
GTCACACACGCTACATGCAA	Dhrsx-Flk-REV	ChIP and CIDOP-qPCR
TCAATCTGTGTCATCAGGTGC	Etv5-In-FOR	ChIP and CIDOP-qPCR
TGCTGATCTCGGGCAGTTTT	Etv5-In-REV	ChIP and CIDOP-qPCR
AGTGAGGGTAGCCTGTAGGG	Etv5-Flk-FOR	ChIP and CIDOP-qPCR
GGTGAGCCACAAGCAGGTAT	Etv5-Flk-REV	ChIP and CIDOP-qPCR
GCCCATCCAGAACCTGCATA	Il3ra-In-FOR	ChIP and CIDOP-qPCR
TGCCCCTCACCCAGACAAA	Il3ra-In-REV	ChIP and CIDOP-qPCR
TCCACCAGGCCTCCAGAATA	Il3ra-Flk-FOR	ChIP and CIDOP-qPCR
TTTGTTGGCCACGTCTCCTT	Il3ra-Flk-REV	ChIP and CIDOP-qPCR
GCACTATGTTCCCCTGCCTT	IntergenicDomain-FOR	ChIP and CIDOP-qPCR
ACTCCAGGCATTACCCGAGA	IntergenicDomain-REV	ChIP and CIDOP-qPCR
GCACCCTCAAAGCCTATCTTA	IAPs-FOR	ChIP and CIDOP-qPCR
TCCCTTGGTCAGTCTGGATTT	IAPs-REV	ChIP and CIDOP-qPCR
GCCTCCAGAGTTTCACTCGT	Csrnp1-FOR	ChIP and CIDOP-qPCR
CGAGGCCAAAAACGCCAAT	Csrnp1-REV	ChIP and CIDOP-qPCR
CACCATGTATCGAGAGGGGC	Etv5-mRNA-FOR	Northern-blot
TCCGGGAAGGCCATAGAGAA	Etv5-mRNA-REV	Northern-blot
AGGTGCTGGTTGTAGGAACG	Etv5-Domain-FOR	Northern-blot
GCCTAACTCTGTTGGCGTCT	Etv5-Domain-REV	Northern-blot
CACCGCCGGCCATATACTGATAACA	SETD2-gRNA-FOR	CRISPR/Cas9 gRNA
AAACTGTTATCAGTATATGGCCGCC	SETD2-gRNA-REV	CRISPR/Cas9 gRNA
CACCGCTCTGAATCGGTTGCGCCT	NSD1-gRNA-FOR	CRISPR/Cas9 gRNA
AAACAGGCGCAACCGATTCAGAGC	NSD1-gRNA-REV	CRISPR/Cas9 gRNA
CACCGCTCTCAATCTCCCCGAAAT	NSD2-gRNA-FOR	CRISPR/Cas9 gRNA
AAACATTTCGGGGAGATTGAGAGC	NSD2-gRNA-REV	CRISPR/Cas9 gRNA
CACCGGTCATCTCGATCCGAAGAG	NSD3-gRNA-FOR	CRISPR/Cas9 gRNA
AAACCTCTTCGGATCGAGATGACC	NSD3-gRNA-REV	CRISPR/Cas9 gRNA
CACCGCTGATACTCAGTGCTCACCG	DualdomainCcny-UpstreamgRNA-FOR	CRISPR/Cas9 gRNA
AAACCGGTGAGCACTGAGTATCAGC	DualdomainCcny- UpstreamgRNA-REV	CRISPR/Cas9 gRNA
CACCGAGGGGGGAGAGCACACACG	DualdomainCcny-DownstreamgRNA-FOR	CRISPR/Cas9 gRNA
AAACTAGTGTGTGCTCTCCCCCCTC	DualdomainCcny- DownstreamgRNA-REV	CRISPR/Cas9 gRNA
CACCGATAACAGGCAGGTGTTTGCC	DualdomainCd200-UpstreamgRNA-FOR	CRISPR/Cas9 gRNA
AAACGGCAAACACCTGCCTGTTATC	DualdomainCd200-UpstreamgRNA-REV	CRISPR/Cas9 gRNA
CACCGCAGGGATTGCACTACGATAT	DualdomainCd200-DownstreamgRNA-FOR	CRISPR/Cas9 gRNA
AAACATATCGTACAATCCCTGC	DualdomainCd200-DownstreamgRNA-REV	CRISPR/Cas9 gRNA
CACCGAGGTGGCTTTGCACTCTTAT	DualdomainMtr-UpstreamgRNA-FOR	CRISPR/Cas9 gRNA
AAACATAAGAGTTGAAAGCCACCTC	DualdomainMtr-Upstream-gRNA-REV	CRISPR/Cas9 gRNA
CACCGGGAGTGATGCTGTGCCATGC	DualdomainMtr-DownstreamgRNA-FOR	CRISPR/Cas9 gRNA
AAACGCATGGCACAGCATCACTCCC	DualdomainMtr-DownstreamgRNA-REV	CRISPR/Cas9 gRNA
CACCGTCTTATAAGGGTCATCTGCC	DualdomainDock9-UpstreamgRNA-FOR	CRISPR/Cas9 gRNA
AAACGGCAGATGACCCTTATAAGAC	DualdomainDock9-UpstreamgRNA-REV	CRISPR/Cas9 gRNA
CACCGGTTTTAAAGTTTTAAAGTTTC	DualdomainDock9-DownstreamgRNA-FOR	CRISPR/Cas9 gRNA
AAACTAATGTCGAAACTTTAAAACC	DualdomainDock9-Downstream-RNA-REV	CRISPR/Cas9 gRNA

GTCCCTGGACCCACGTAAAG	Etv5-Luciferase-FOR	Luciferase repoter assay
GTCCATCCCGGACAAACTGT	Etv5-Luciferase-REV	Luciferase repoter assay
CGCCCTCAGAGTTCTGTTGT	Fermt2-Luciferase-FOR	Luciferase repoter assay
GGCAGGAAGGGAGCAGAAAT	Fermt2-Luciferase-REV	Luciferase repoter assay
GTCTCACAAGACTCAGGCCC	Il3ra-Luciferase-FOR	Luciferase repoter assay
CTAGGCACAGCGGTTTTTGC	Il3ra-Luciferase-REV	Luciferase repoter assay
CTTTCCTGTTCACTCGGGCT	Lemd1-Luciferase-FOR	Luciferase repoter assay
TGCTGCCTGTCCTACCATTG	Lemd1-Luciferase-REV	Luciferase repoter assay
TAGACCCTGCTCGGTGGAAT	Zfp11-Luciferase-FOR	Luciferase repoter assay
AACAAAGAACCATGAGGCTGTT	Zfp11-Luciferase-REV	Luciferase repoter assay
GGGTTCCTTGACATCAGCCA	Ror2-Luciferase-FOR	Luciferase repoter assay
GTTGAAGAGTAGGGTGGCCC	Ror2-Luciferase-REV	Luciferase repoter assay
TAGCATGTGGCTTCACAGGG	Intergenic-Luciferase-FOR	Luciferase repoter assay
TTCCAGCATTCACGGTTCCA	Intergenic-Luciferase-REV	Luciferase repoter assay
AGGTCTAAGGGTGTGCCAGG	H3K9me3only-Luciferase-FOR	Luciferase repoter assay
GCTGGTATCCCCACTCTTTCC	H3K9me3only-Luciferase-REV	Luciferase repoter assay
GGGGTACCACAGGGTTTAGC	H3K36me3only-Luciferase-FOR	Luciferase repoter assay
TCCCAAGCTAGAGGCAAAGC	H3K36me3only-Luciferase-REV	Luciferase repoter assay